Computer-Aided Civil and Infrastructure Engineering **23** (2008) 448–464

INDUSTRIAL APPLICATION

Dynamic Response of a Rollover Protective Structure

David P. Thambiratnam* & Brian J. Clark

School of Urban Development, Faculty of Built Environment & Engineering, Queensland University of Technology, Brisbane, Australia

&

Nimal J. Perera

School of Urban Development, Faculty of Built Environment & Engineering, Queensland University of Technology, Brisbane, Australia
Robert Bird Group, Brisbane, Australia

Abstract: *Roll Over Protective Structures (ROPS) are safety devices fitted to heavy vehicles to provide protection to the operator during an accidental roll over. At present, ROPS design standards require full-scale destructive testing that can be expensive, time consuming, and unsuitable for small companies. More economical analytical methods are not permitted due to a lack of understanding of post yield behavior and the energy absorption capacity of ROPS. To address this, a comprehensive research project was undertaken to investigate ROPS behavior using analytical techniques supported by experiments. This article presents the dynamic impact analysis of a bulldozer ROPS using calibrated finite element models. Results indicate that (1) ROPS posts have significant influence on the energy-absorbing capacity, (2) dynamic amplifications in energy could be up to 25%, (3) stiffer ROPS cause high peak decelerations that may be detrimental to the operator, and (4) analytical techniques may be used for evaluating ROPS performance.*

1 INTRODUCTION

Heavy vehicles that are used in the rural, mining, and construction industries are susceptible to rollovers as they have a high center of gravity and commonly operate on sloping and uneven terrain. A steel moment-resisting frame with either two or four posts is usually attached to these vehicles above the operator's cabin for protection during rollovers. This safety device is called a Rollover Protective Structure (ROPS) and its role is to absorb some of the kinetic energy (KE) of the rollover, while maintaining a survival zone for the operator. The design and analysis of ROPS is complex and requires dual criteria of adequate flexibility to absorb energy and adequate stiffness to maintain a survival zone around the operator.

Evaluation techniques used in the current Australian standard for earth moving machinery protective structures AS2294–1997 are simplified and involve full-scale destructive testing of ROPS subjected to static loads along their lateral, vertical, and longitudinal axes. The standard is performance based, with certain force and energy absorption criteria that are derived from empirical formulae related to the type of machine and operating mass. Deflection restrictions are also employed to enable a survival space known as the dynamic limiting volume (DLV) to be maintained for the vehicle operator. These simplified provisions provide design guidelines that will substantially improve the operator's chances of survival during an accidental rollover. This form of certification can be time consuming and extremely expensive

*To whom correspondence should be addressed. E-mail: *d.thambiratnam@qut.edu.au*.

as establishing the force and energy criteria can involve large loads that may therefore require the use of a specialized testing facility.

Certification of ROPS by more economical analytical modeling techniques is currently not permitted by ROPS standards for earthmoving machinery both in Australia and internationally. Reasons for the exclusion are attributed to a lack of knowledge and research information on the behavior of these structures in the post yield region and their energy-absorption capacity. Preliminary research has shown promise for the use of analytical techniques to model the nonlinear response of ROPS. These analytical methods were very simplified and involved the use of elasto-plastic beam elements to simulate the behavior of ROPS subjected to a static lateral load. In recent years, substantial advances have been made in both computational power and the implementation of advanced element types in Finite Element (FE) techniques that can accurately model and predict the nonlinear response of structures, particularly in the post yield region. Research carried out on ROPS behavior using analytical and experimental techniques include those of Clark et al. (2006a,b), Kim and Reid (2001), Tomas et al. (1997), Swan (1988), and Huckler et al. (1985).

A comprehensive research project was undertaken at the Queensland University of Technology to investigate ROPS behavior using computer simulations supported by experiments to (1) enhance our understanding of ROPS behavior, (2) improve energy absorption and safety, and (3) generate research information to facilitate the development of analytical techniques for design and evaluation that may lessen the need for destructive full-scale testing (Clark, 2006a).

This article treats the dynamic response of the ROPS model for a K275 bulldozer, using calibrated FE models. The experimental testing and calibration of the compute model of this particular ROPS model are reported elsewhere (Clark, 2006a,b). The dynamic impact loads are characteristic of those that are experienced during the sidewards rollover of a vehicle on a firm slope. A simplified method based on a conservation of angular momentum approach reported by Watson (1967) is used to estimate the dynamic impact parameters for the ROPS during a sidewards overturn. The explicit FE code LS-Dyna v970 was used to conduct the necessary dynamic impact modeling for rollover impacts on firm slopes with inclinations of 15°, 30°, and 45°. The influence of controlling variables such as ROPS stiffness, impact velocity, and duration and roll slope angle on the dynamic response of the ROPS was studied. The results are compared with those from previous static analysis to establish the effect of possible dynamic amplifications and the adequacy of current standard provisions.

1.1 Dynamic finite element analysis

Rollover simulation using FE analysis has received little attention from researchers. Chou et al. (1998) highlighted that the major difficulty associated with using FE for rollover analysis was the large simulation time required to capture the event accurately. In direct parallel to this, Klose (1969) also emphasized that the rollover process was extremely difficult to model as it involved the complex interaction of numerous parameters that influenced the behavior of the rolling vehicle. In the open literature, the FE modeling of rollover protective structures under dynamic loading has been limited to research performed by Tomas et al. (1997) and Harris et al. (2000). The work performed by Harris (2000) examined the rearward rollover of a tractor whereas Tomas's research used the program MADYMO to study the effect of ROPS stiffness and occupant restraint during the sidewards rollover of an earthmoving machine. Although the modeling techniques employed by each of these authors have assisted with assessing the performance of ROPS under simulated dynamic impact loads, little comparison has been made with reference to the adequacy of the static loading procedures adopted in current ROPS standards and the possible dynamic amplifications that may take place during such loading conditions. With these views in mind the simplified procedure proposed by Watson (1967) is used as a basis for a dynamic impact study to investigate the influence of critical parameters that control the response behavior of ROPS subjected to such loading conditions.

2 ROPS FOR K275 BULLDOZER

The K275 bulldozer is a crawler type dozer with a gross vehicle weight of approximately 50 tons commonly used in the construction and mining industries for earthmoving purposes. Rollover protection for the occupant is afforded through a two post rollbar type ROPS, which is shown in Figure 1.

This ROPS is primarily a fixed base portal frame, consisting of two posts and a beam, rigidly connected to the chassis of the vehicle. In addition to the ROPS, an additional roof canopy section known as the Falling Object Protective Structure (FOPS) , is incorporated to provide protection to the operator under falling objects. In this study, the FOPS, which is a separate detachable structure, was omitted. The overall geometry of the full-scale K275 ROPS model was established from site measurements taken at the manufacturer's storage yard. Appropriate RHS/SHS member sizes were selected so that the ROPS would possess sufficient strength and energy absorption characteristics that would enable it to successfully pass the requirements of the Australian Standard.

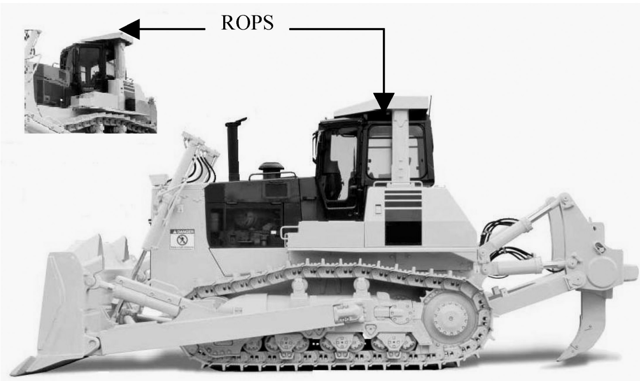

Fig. 1. K275 bulldozer with ROPS.

2.1 Half-scale ROPS model

Previous research by Srivastava et al. (1978) has shown that principles of similitude modeling could be successfully applied to ROPS testing techniques, and could lead to large-scale economic savings. Based on the research findings of these authors the principles of similitude were applied to the K275 bulldozer ROPS to lessen fabrication costs and reduce the magnitudes of the test loads to be applied to the ROPS. Reduction in the magnitudes of the loads was essential as a full-scale test of ROPS for a vehicle such as this was extremely large and would require the use of an extensive laboratory testing facility. A scaling factor (for size) was then selected between the model and prototype that gave rise to the scaling factors of 1/8 for energy absorbed under lateral load, 1/4 for loads, and 1/2 for deflections. A half-scale model of the K275 ROPS with length 1,000 mm, height 900 mm, and section properties 125 × 75 × 5 mm for the posts and 125 × 125 × 5 mm for the beam, was designed and fabricated and subjected to the loading and energy requirements of AS2294–1997. The member types used for the ROPS consisted of 350 grade RHS with full penetration butt-welded moment-resisting connections. The half-scale K275 ROPS model was experimentally tested under the required lateral, vertical, and longitudinal loads (Clark, 2006a). The load and energy magnitudes established from AS2294.2–1997 were modified to take into account the similitude relationships established for this model. Strain and deflection measurements were recorded for each loading sequence.

The experimental testing was followed by FE analysis of the half-scale ROPS model under the same loads, using the program ABAQUS standard v6.3. Scaling laws from the similitude study along with the program MSC Patran were used to develop the necessary geometry for the FE model.

Figures 2 and 3 show the experimental testing of the ROPS model under lateral load and the FE model of the same ROPS, respectively. The rectangular portion (in lighter shade) at the top right-hand post in the FE model shows the rigid body used to apply the dynamic impact loading described later on in the article. The lateral load deflection plots obtained experimentally and from the FE analysis shown in Figure 4 demonstrate excellent agreement between the two sets of results. The variation of the stress with load at the base of the ROPS post (a critical region), also showed excellent agreement between the experimental and analytical results (Clark, 2006a). This calibrated FE ROPS model was used for the dynamic analysis under lateral impact loads.

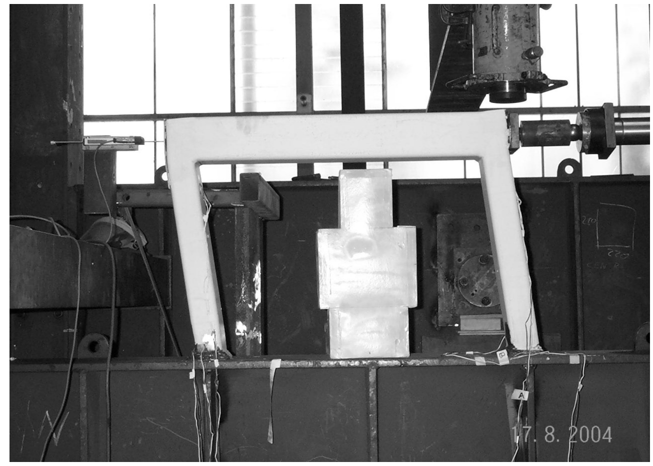

Fig. 2. Lateral load testing of K275 ROPS.

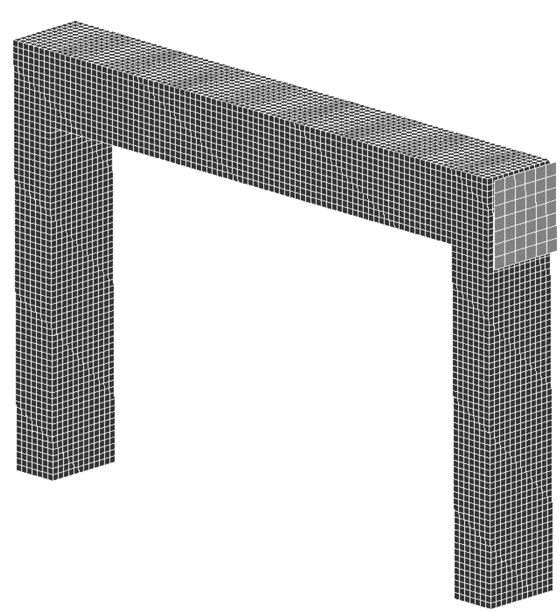

Fig. 3. Finite element model of K275 ROPS.

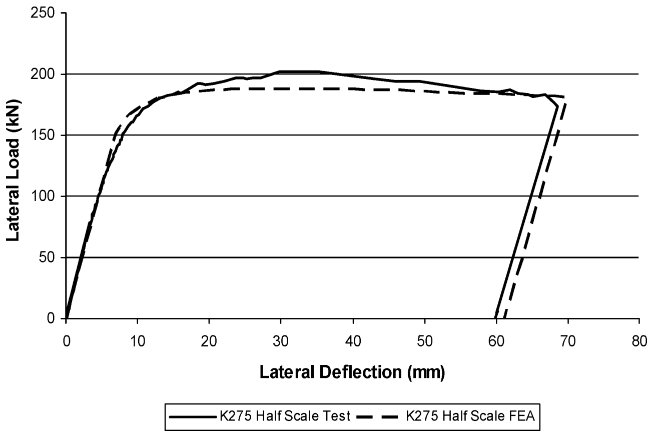

Fig. 4. Lateral load deflection response from experiment (LVDT 1) and FEA.

3 DEVELOPMENT OF PARAMETERS FOR DYNAMIC IMPACT ANALYSIS FOR K275 BULLDOZER

Watson's procedure (1967) based on conservation of angular momentum, is used to determine the impact parameters for the RPOS model for roll slope inclinations of $\alpha = 15°, 30°$, and $45°$. The simplifying assumptions of this procedure include: neglecting forward velocity, use of a two-dimensional vehicle model, assuming the vehicle's center of gravity to be directly above the point of rotation at the wheel just before the roll, and treating the vehicle as a rigid body that falls sideways freely under gravity with no change in angular momentum about the point of impact.

3.1 Derivation of K275 bulldozer rollover parameters

Figures 5a–c illustrate the three stages in the rollover of a vehicle, which initially rolls about A, then about B, and finally makes impact with the ground at D at which it also rolls.

Loss in potential energy = Gain in KE

$$Mg\sqrt{x^2+y^2}\left[1-\sin\left\{\tan^{-1}\left(\frac{y}{x}\right)-\alpha\right\}\right] = \frac{1}{2}M(k^2+x^2+y^2)\,\omega_A^2. \quad (1)$$

From which

$$\therefore \omega_A = \sqrt{\frac{2g(x^2+y^2)\left[1-\sin\left\{\tan^{-1}\left(\frac{y}{x}\right)-\alpha\right\}\right]}{k^2+x^2+y^2}}. \quad (2)$$

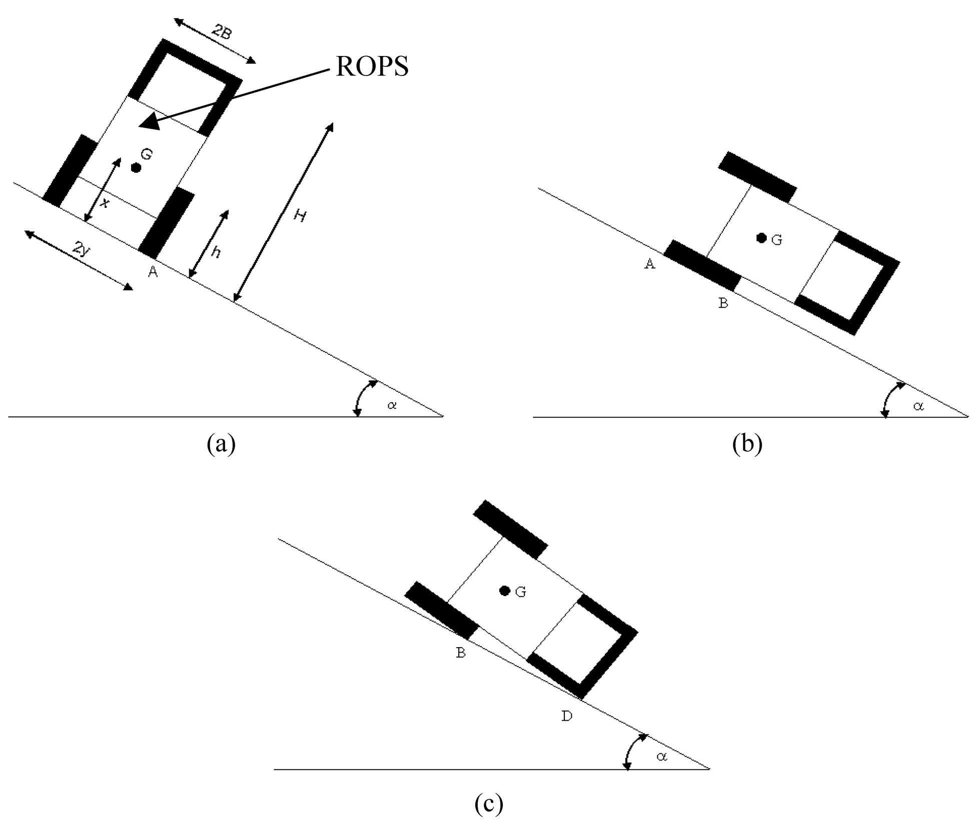

Fig. 5. (a) Initial rollover conditions, (b) impact on wheel at point B, and (c) impact on ROPS at point D.

Angular momentum of bulldozer about B after impact =

$$\mathrm{I_B}\omega_\mathrm{B} = M\omega_b[k^2 + (h-x)^2 + y^2]. \quad (3)$$

Gain in KE between B and D

$$= \frac{M}{g}\sqrt{(h-x)^2+y^2}\left[\cos\left\{\tan^{-1}\left(\frac{h-x}{y}\right)-\alpha\right\} - \cos\left\{\alpha+\tan^{-1}\left(\frac{y-b}{H-h}\right)-\tan^{-1}\left(\frac{h-x}{y}\right)\right\}\right] \quad (4)$$

Then total KE as the ROPS reaches the ground at D

$$= \tfrac{1}{2}\mathrm{I_B}\omega_\mathrm{B}^2 + \text{Gain in KE between B and D} = \tfrac{1}{2}\mathrm{I_B}\omega_\mathrm{C}^2, \quad (5)$$

where ω_C is the angular velocity of the vehicle just before impact at D.

By equating the angular momentum before and after the impact at point D, it is possible to derive the angular velocity ω_D of the vehicle after impact at D and hence the KE of the system after impact is, as given by,

$$I_G\omega_C + M\omega_C\sqrt{(h-x)^2+y^2}\times DK \quad (6)$$

$$= I_D\omega_D = M\omega_D[k^2 + B^2 + (H-x)^2] \quad (7)$$

where

$$\mathrm{DK} = \sqrt{(h-x)^2+y^2} + \sqrt{(H-h)^2+(y-B)^2} \times \sin\left[\tan^{-1}\left(\frac{h-x}{y}\right)-\tan^{-1}\left(\frac{y-B}{H-h}\right)\right]$$

In the above expressions, x, y, h, H, and B are vehicle dimensions as shown in the Figures 5a–c, k is its radius of gyration about the centroid, ω_i angular velocity about the point $i(= A, B, C, D, \text{ or } G)$ and I_i the moment of inertia about i.

3.2 Determination of moment of inertia of vehicle

The moment of inertia (I_G) about the vehicle's center of gravity, is a parameter that is not readily available from the vehicle manufacturer. To overcome this problem a two-dimensional rectangular approximation of the vehicle was made, dimensions of which are outlined in Figure 6. Using this rectangular approximation for the vehicle and assuming that there is an even mass distribution and that the centroid of the vehicle is located 1.45 m from the ground, the moment of inertia about the vehicle's centroid may be estimated using the following equation:

$$I_G = \frac{1}{12}M(a^2+b^2) + Mc^2. \quad (8)$$

The terms a and b represent the length and width of the rectangle whereas M and c represent the mass of

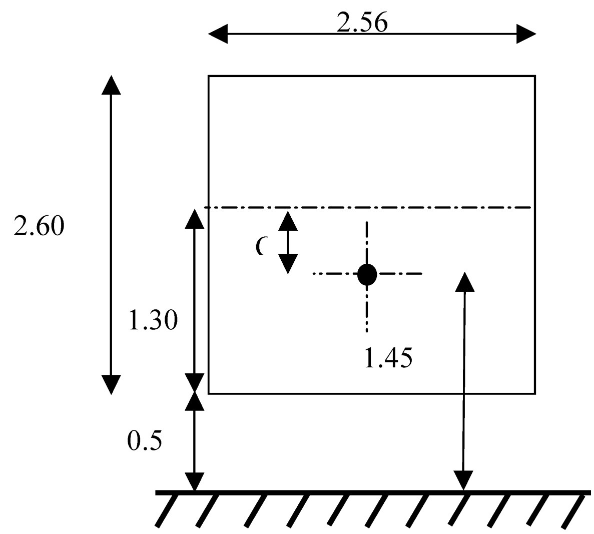

Fig. 6. Rectangular approximation of K275 bulldozer for moment of inertia calculation.

the vehicle and its distance from the geometrical center, respectively. Using the values of $a = 2.60$ m, $b = 2.56$ m, $c = 0.35$ m, and $M = 49{,}850$ kg for the K275 bulldozer, the moment of inertia of the vehicle about the centroid can be approximately calculated as 62,000 kgm^2. This value compares well with the value of 60,000 kgm^2 obtained by Cobb (1976) for a 50-ton tractor.

3.3 Kinetic energies and velocities for different roll slope angles

The equations derived in the previous sections were applied to the K275 ROPS for roll slope angles of 15°, 30°, and 45°. Table 1 shows a summary of the results obtained for the kinetic energies and angular velocities at different stages of the roll. The last row gives the velocity of impact of the ROPS with the ground during a sideward roll over.

3.4 Energy absorption by soil

The amount of energy absorbed by the soil was derived from information based on research performed by Kacigin and Guskov (1968). These authors suggested that the force developed in the soil normal to the ground slope could be approximated by the following equation:

$$F_g = Ap\tanh\left(\frac{K}{p}\Delta\right), \quad (9)$$

where A is the area of contact, K the coefficient of volumetric compression, p the bearing capacity of the soil, and Δ the maximum soil deflection. For the present investigation, these parameters were set at $\Delta = 100$ mm, $K = 20.7$ kg/cm^3, and $p = 46.2$ kg/cm^2, based on information provided by Cobb (1976) and representative of

Table 1
K275 dynamic rollover parameters

Property	*Units*	*Ground slope (α)* 15°	30°	45°
(1) KE_A before impact	J	524,748	758,301	1,004,635
(2) ϖ_A	Rad/s	2.05	2.47	2.84
(3) ϖ_B	Rad/s	1.94	2.34	2.69
(4) KE_B after impact	J	272,814	394,237	522,305
(5) KE_{BD} gain	J	23,015	44,968	63,858
(6) KE_D total before impact	J	295,830	439,206	586,164
(7) ϖ_C	Rad/s	2.02	2.47	2.85
(8) KE_D after impact	J	87,193	129,452	172,767
(9) ϖ_D	Rad/s	0.64	0.78	0.91
(10) Energy absorbed by soil	J	25,717	25,717	25,717
(11) Energy absorbed by ROPS = (6)-(8)-(10)	J	182,919	284,037	387,679
(12) Translational velocity at impact	m/s	2.71	3.37	3.94

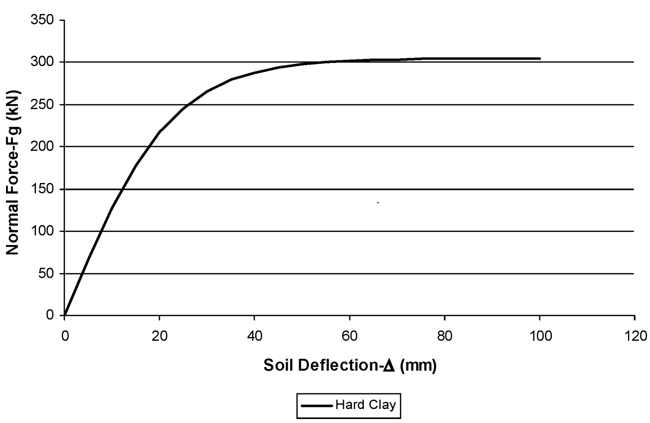

Fig. 7. Force-deflection behavior for hard clay soil.

average values for firm clay soils. These parameters were used in Equation (9) to construct the load deflection response profile for the soil as shown in Figure 7. The energy absorbed by the soil was then determined by calculating the area under this curve. This amount was subtracted from the estimated amount of energy that the ROPS must absorb during the impact, resulting in a slightly reduced translational velocity at impact.

4 DEVELOPMENT OF A DYNAMIC FE MODEL FOR K275 BULLDOZER ROPS

A full-scale FE model of the K275 ROPS of length 2,000 mm and height 1,800 mm, which was treated earlier (Clark, 2006a) was developed and subjected to dynamic impact forces that were characteristic of those sustained by the ROPS during the first impact of a sidewards rollover. The section properties of the ROPS members were 350 grade 150 × 250 × 10 mm RHS for the posts (initially) and 350 grade 250 × 250 × 12 mm RHS for the beam. Subsequently the post sizes were varied to study the influence of the post stiffness on the ROPS response as described in Section 5. During a rollover, the impact between the ground surface and the ROPS results in energy absorption by both the ROPS and the ground. To simplify the modeling procedure, the ground surface was idealized as a rigid body that was able to transfer the estimated rollover KE into the ROPS. This KE transfer was performed by assigning the vehicle's mass to a rigid body and moving it laterally into the ROPS with a prescribed translational velocity. The velocity of the rigid body was adjusted to account for the energy absorbed by the ground surface during the impact as discussed above for a firm clay surface. The KE imparted to the ROPS was derived from the results obtained using Watson's procedure for each roll slope angle, and summarized in Table 1.

The geometry and mesh definition necessary to accurately model the ROPS were developed using the pre-processor MSC Patran, in conjunction with the LS-DYNA pre-processor Femb v28.0. The surface geometry of the ROPS was defined with reference to the mid thickness section of each member and was meshed using quadrilateral shell elements. The surface definition of the model predominantly has two major parts, the ROPS and the rigid body at the top right-hand post shown in lighter shade in Figure 3. Corner radii were omitted in the ROPS model as they had minimal global influence and to simplify the connection between the post and the beam.

The Hughes–Liu shell element was chosen to model the response behavior of the K275 ROPS under the established loading conditions. This particular element type is a reduced integration, large strain, shell element that consists of four nodes with six degrees of freedom per node. Selection of this element was based on its simplistic formulation and overall computational efficiency. The mesh density chosen for the ROPS was 20 mm and the shell thicknesses that were implemented throughout the model were 10 mm for the posts and 12 mm for the beam. All nodes were equivalenced particularly at the connection region between the posts and the beam to permit uniform stress transfer throughout these regions.

The performance of ROPS is based primarily on its ability to absorb energy, which is most commonly implemented through the formation of plastic hinges at specified locations within the structure. The selection of an adequate material model is vital to the performance of the ROPS and such a model must be capable of accounting for the nonlinear stress/strain behavior of the chosen material. To accurately model this behavior, the LS-DYNA nonlinear material model MAT_PIECEWISE_LINEAR_ PLASTICITY was selected. This constitutive relation requires that the stress/strain behavior of the steel be included in the form of a true stress versus plastic strain curve. The required material properties were calculated using Equation (10a,b) and were based on uni-axial tensile testing of coupons cut from the 350 grade RHS/SHS used in the ROPS model that was experimentally tested (Clark, 2006a).

$$\sigma_{Ttrue} = \sigma_{Eng}(1 + \varepsilon_{Eng}) \tag{10a}$$

$$\varepsilon_{Plastic} = \ln(1 + \varepsilon_{Eng}) - \frac{\sigma_{True}}{E}. \tag{10b}$$

Figure 8 shows the true stress versus plastic strain relationship that was incorporated into LS-DYNA for all analyses. In addition to this material density $\rho = 7{,}850$ kg/m^3, elastic modulus E = 200,000 Mpa, and Poisson's ratio $\nu = 0.3$ were assumed.

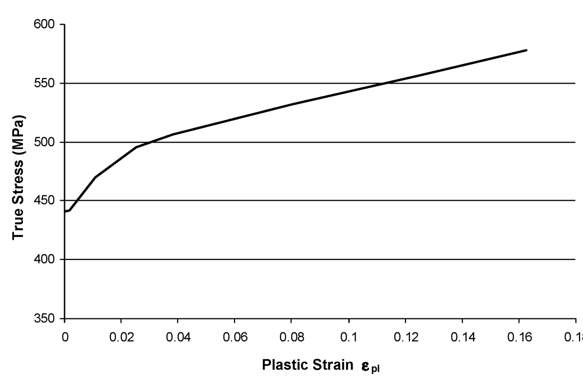

Fig. 8. True stress vs. plastic strain distribution for ROPS material.

The influence of strain rate effects on the dynamic response of the steel RHS/SHS used in the fabrication of ROPS was incorporated into the LS_DYNA material model by adopting the Cowper Symonds constitutive relation. Cowper Symonds coefficients of $D = 950$ s^{-1} and $q = 4$ were chosen for the model based on research conducted by Johnson (2001) who used these parameters for a similar impact study involving 350 grade RHS. The boundary conditions applied to the model were designed to simulate full base fixity at the base perimeter nodes of the ROPS posts. An acceleration field was also applied to the model in the downward vertical direction to simulate the effects of gravity on the model.

The loading procedure for the impact study involved the use of a rigid impacting surface that was modeled as a rectangular plane of dimensions 250 mm wide by 280 mm high and 10 mm thick. These dimensions were chosen based on a width equivalent to that of the ROPS post and on the assumption that approximately 20% of the height of the ROPS post would come into contact with the ground during a rollover. The impacting body was meshed with 40-mm density Hughes–Liu shell elements and assigned the LS-DYNA material type 20 MAT_RIGID, to reduce the computational time required to perform the necessary analyses. The impacting body was constrained globally about all the degrees of freedom with the exception of the translation along the horizontal direction to enable it to translate in the direction of the applied lateral velocity. To enable the impacting body to transfer the correct amount of KE to the ROPS, it was assigned a mass equal to that of the K275 bulldozer. This mass was distributed evenly throughout the body by assigning an appropriate mass density. The rigid impacting body was given initial translational velocities of 2.71, 3.37, and 3.94 m/s to represent the impact velocities that would occur for rollovers on slopes with inclinations of 15°, 30°, and 45°, respectively.

The contact definition between the impacting surface and the ROPS was modeled using the LS-DYNA contact type AUTOMATIC_NODES_TO_SURFACE. For each model, the impacting body was selected as the master surface, whereas the ROPS was selected as the slave surface. The static and dynamic coefficient of friction between the two surfaces was set to 0.6, which was in accordance with the value chosen by Cobb (1976) for a similar numerical rollover study. Other variables required by LS-DYNA for contact definition were set to their default values. No self-contact was defined for any part of the ROPS, as it was found from visualization of the deformed ROPS structure that no elements came into contact with each other during the analysis.

Four different forms of output were requested from each FE model. (1) DATABASE_BINARY_D3PLOT to view the results of the model using the post-processor eta/PostGL, (2) DATABASE_GLSTAT to obtain the global energy data during the analysis that included the kinetic, internal, sliding, and total energy of the system, (3) DATABASE_NODOUT to track the displacement, velocity, and acceleration of a node located at the centroid of the rigid body, and (4) DATABASE_SPCFORC to record the reaction forces at the supports of the ROPS during the analysis that will be used in the development of the load deflection profile for the ROPS. All results were graphed and visualized using the programs ETA PostGL and ETAGraph, respectively.

Fig. 9. Von Mises stress distribution and plastic hinges during impact.

5 RESULTS OF DYNAMIC IMPACT ANALYSIS

To develop a comprehensive understanding of the ROPS behavior under impact loads and its energy absorption capabilities, a detailed numerical investigation was performed that involved adjusting the stiffness of the ROPS posts. To achieve the required stiffness variation between the models, post sizes of $120 \times 250 \times 10$, $150 \times 250 \times 10$, $200 \times 250 \times 10$, and $250 \times 250 \times 10$ were chosen, along with the constant beam size of $250 \times 250 \times 12$ mm. Each model was analyzed using LS-DYNA for simulated impacts on firm slopes with inclinations of 15°, 30°, and 45° and involved the movement of a rigid impacting surface into the side face of the ROPS model with an appropriate velocity that corresponded to the angle of inclination of the roll slope, as given in Table 1.

5.1 Formation of plastic hinges

During the initial contact phase between the two bodies, the rigid surface began to impart the stored KE to the ROPS. This transfer of energy resulted in the ROPS deforming appreciably and was characterized by the formation of plastic hinges at the top and base of each post of the ROPS. Figure 9 shows the Von Mises Stress distribution in the $150 \times 250 \times 10$ mm post ROPS for 30° roll slope angle and confirms the presence of yielding at the hinge locations at the top and base of the posts. The response behavior of the ROPS during this phase was characteristic of the collapse mode displayed by a typical fixed base frame subjected to a static sidewards load and was very similar to the behavior displayed by the same ROPS model studied earlier under static loads (Clark, 2006a). Other ROPS models displayed analogous behavior.

5.2 Velocity and peak deceleration response

The velocity versus time response of the rigid surface was measured during the impact at a node located at the rigid surface's centroid. Results showed a linear reduction in the velocity of the rigid surface during the impact as the rigid surface was brought to rest from the initial velocity. The contact time between the ROPS and the impacting surface required to dissipate the KE depends on the stiffness of the ROPS and the velocity of the impacting surface. The contact time decreased with the stiffness of the ROPS (posts) and increased with roll slope angle (Clark, 2006a) and in the present investigation varied from 80 ms for the stiffest ROPS (with $250 \times 250 \times 10$ mm posts) and roll slope angle 15° to 280 ms for the least stiff ROPS (with $120 \times 250 \times 10$ mm posts) and roll slope angle 45°. For a stiffer ROPS impacting a firm surface, the contact time is small, which will result in the transfer of large forces and peak decelerations into the ROPS. When the stiffness of the ROPS is reduced, the contact time will increase and will result in the transfer of much smaller forces and peak decelerations into the ROPS. This response behavior is more desirable for the occupant, but will be characterized by larger deformations, which might encroach upon the operator's cabin. The dual design criteria of adequate stiffness and energy absorption capability of the ROPS are thus evident.

The variations in the peak deceleration of the rigid surface with time were also monitored at the centroid of the rigid surface during impact and the results are shown in Figures 10a–d. These figures show that the initial response was characterized by significant fluctuations and large peak deceleration readings. The duration of the fluctuations decreased with ROPS stiffness, whereas the peak decelerations increased with ROPS stiffness. These initial peak decelerations vary from about $6g$ for the stiffest ROPS to about $4g$ for the least stiff ROPS and were due to the initial stiff response of the ROPS in the elastic region as the rigid surface came into contact

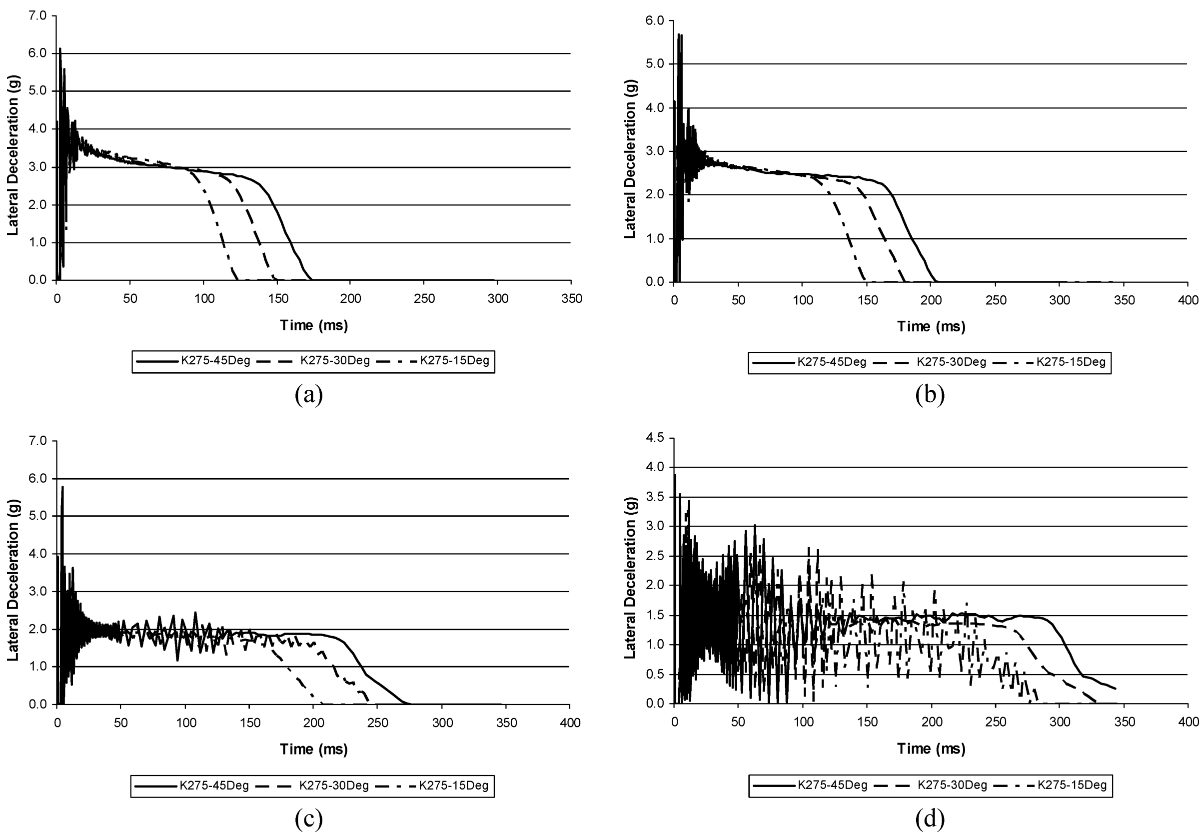

Fig. 10. (a) Acceleration vs. time response K275 ROPS—250 × 250 × 10 posts, (b) acceleration vs. time response K275 ROPS—200 × 250 × 10 posts, (c) acceleration vs. time response K275 ROPS—150 × 250 × 10 posts, and (d) acceleration vs. time response K275 ROPS—120 × 250 × 10 posts.

with the ROPS. As the structure started to yield and the plastic hinge formation throughout the structure became more pronounced, the deceleration response of the rigid surface stabilized to approximate mean values that varied from 3*g* for the stiffest ROPS to 1.5*g* for the least stiff ROPS.

5.3 Load deflection response and energy absorption

Figures 11a–d show the load deflection responses of the ROPS. The magnitude of the load for each time step was calculated through summation of the base reaction forces measured in the direction of the applied impact. The deflection of the ROPS was measured by monitoring the displacement of the rigid impacting surface as it came into contact with the ROPS. All the ROPS models displayed similar response, with a higher force and lower deflection demand for the higher stiffness ROPS. This result was expected, as the collapse load for a ROPS frame is directly related to the post stiffness and the stiffer ROPS is able to absorb energy with less deflection, as the force demand is higher. The similarity in the shape of each graph, irrespective of the angle of inclination of the roll slope, is also noticeable. Although the energy demand placed on ROPS increases with increasing roll slope inclination, it appears to have minimal influence on the initial part of the load deflection response for a given ROPS configuration. It also appears that the influence of strain rate effects for the narrow velocity range covered in this study is reasonably uniform.

The energy absorbed by the ROPS can be determined from the area beneath the load deflection response profile. This quantity of energy absorption should be approximately equivalent to the KE imparted to the ROPS by the rigid surface. The KE versus time and energy absorption versus time response profiles for the impacts are shown in Figures 12a–d. The KE for each case decreases with time although the energy absorbed increases with time. As predicted, the two curves for each case are a reverse mirror image of one another with some minor variations taking place due to a small percentage of energy being dissipated through friction. These energy absorption values are higher than those under static analysis. For example, in the case of the 150 × 250 × 10 mm ROPS and a roll slope angle of 30°, Figure 12c indicates that the

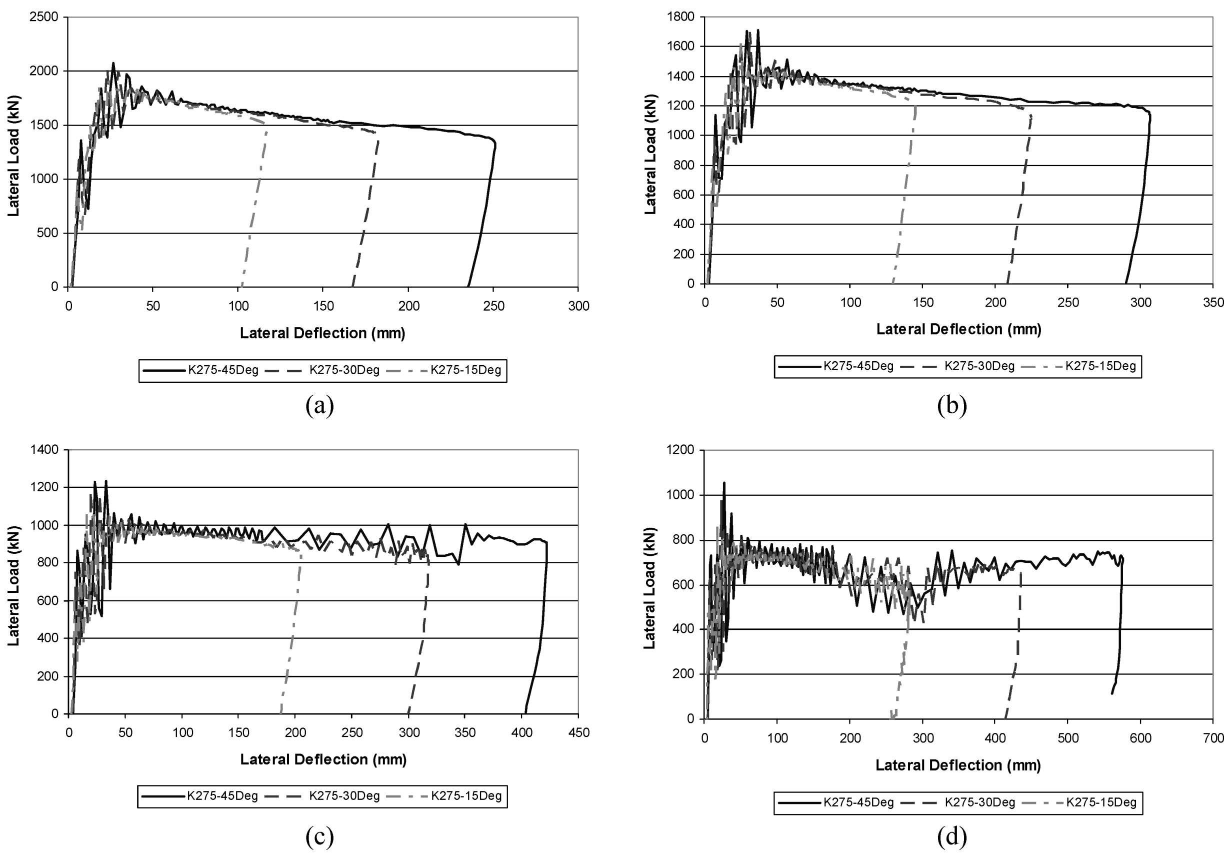

Fig. 11. (a) Load deflection response K275—250 × 250 × 10, (b) load deflection response K275—200 × 250 × 10, (c) load deflection response K275—-150 × 250 × 10, (d) load deflection response K275—120 × 250 × 10.

ROPS was required to absorb approximately 250,000 J of energy, which is almost three times the amount required from AS2294.2 (1997). The difference between these two energy absorption levels suggests that there are some distinct discrepancies between the two approaches. As mentioned previously the exact philosophy used to develop the code requiring energy absorption levels is difficult to quantify, whereas the dynamic loads used in the present study were established from a simplified mathematical model.

5.4 Elastic rebound energy

Current ROPS standards give designers little guidance on how to adequately proportion a ROPS to meet their specified requirements. The many ROPS configurations investigated analytically in the QUT research project (Clark, 2006a), suggested that a carefully proportioned ROPS with sufficient stiffness about the lateral direction may be able to satisfy the requirements of the standard adequately. The term "may" has been used wisely here, as it is extremely important that the ROPS members be proportioned so that they will have sufficient strength to withstand the subsequent vertical and longitudinal loading requirements of the standard. Designers and manufacturers commonly develop excessively stiff ROPS to avoid premature failure and subsequent retesting. The reason for this is driven by economical constraints as the nature of ROPS standards currently do not permit the use of analytical testing procedures for the certification of ROPS. Through carrying out the dynamic impact simulations on the above-mentioned ROPS model, it has been discovered that increased ROPS stiffness leads to a shorter contact time and the development of larger reaction forces and consequently the transfer of increased peak decelerations to the vehicle's occupants.

It is well understood that each of these response parameters are undesirable and may jeopardize an occupant's chances of survival during a rollover. Carney (1993) has suggested that unacceptably high decelerations can be responsible for severe occupant injury during vehicle collisions. In addition to this, the use of an overly stiff ROPS will also result in the generation of more elastic rebound energy, which in the case of a rollover may lead to multiple revolutions of the vehicle after the initial impact. Lu and Yu (2000) suggested

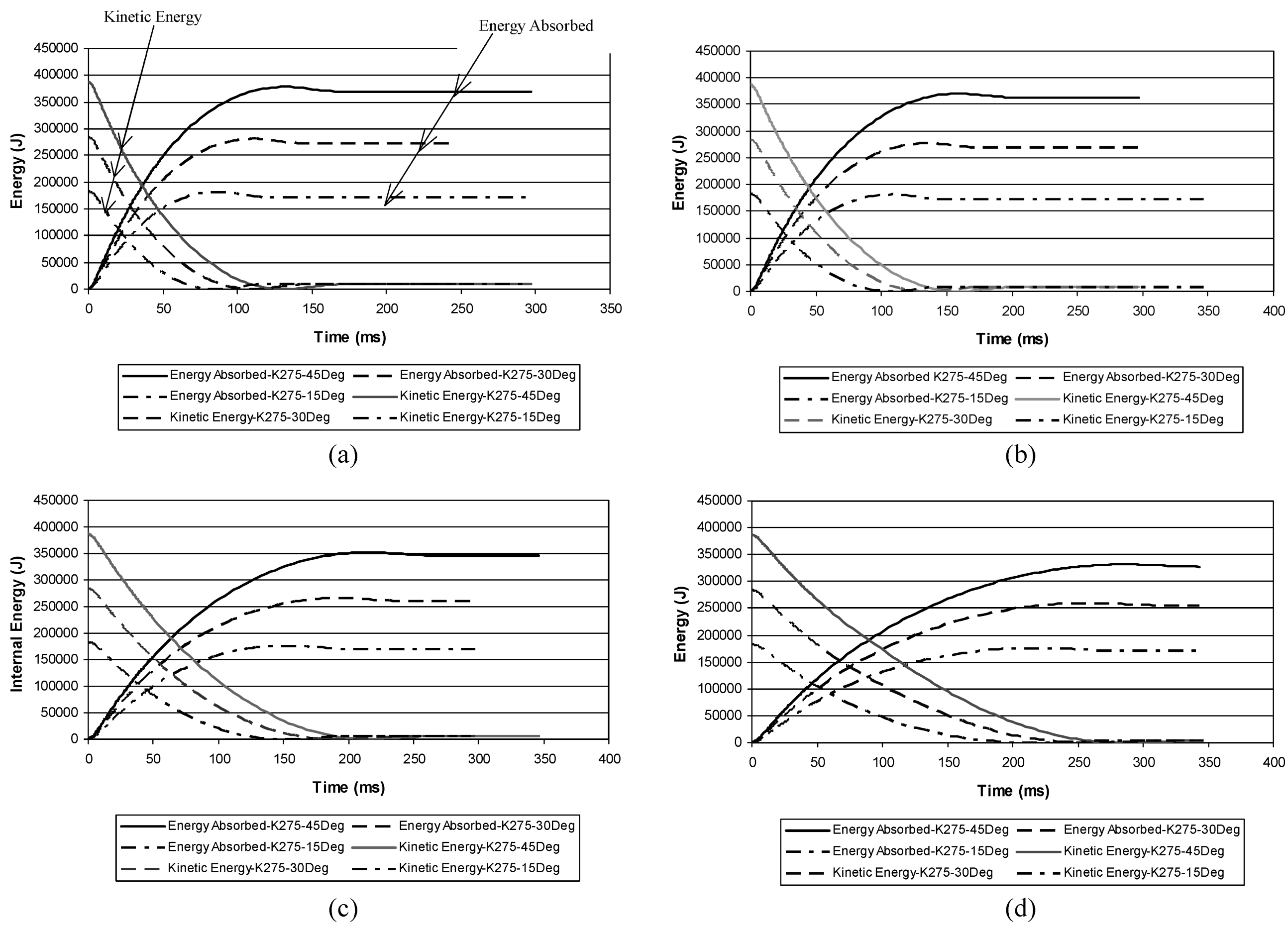

Fig. 12. (a) Energy vs. time response of K275 ROPS—250 × 250 × 10 mm, (b) energy vs. time response of K275 ROPS—200 × 250 × 10 mm, (c) energy vs. time response of K275 ROPS—150 × 250 × 10 mm, and (d) energy vs. time response of K275 ROPS— 120 × 250 × 10 mm.

that during an impact, the recoverable elastic energy may lead to further injury to the occupants of vehicles as well as the structure that is being protected and to illustrate this concept they proposed a simple model based on the collision of a vehicle with an elastic spring. During such a collision, the spring would compress, which would cause the vehicle to decelerate and transfer its KE of the impact into stored elastic strain energy in the spring. Under a situation such as this, where no plastic deformation is able to take place, the elastic strain energy will be released once the maximum elastic deflection capability of the spring has been reached. At this stage, the stored elastic strain energy will be converted back into KE and will result in the acceleration of the vehicle in the opposite direction. Under a situation such as this, the authors suggest that the initial deceleration followed by an acceleration in the opposite direction may cause severe injuries to the vehicle's occupants. The simplified elastic spring analogy proposed by Lu and Yu (2000) was used to address the adequacy ROPS performance during the impact simulations. Figure 13 shows the variation in the elastic rebound energy with the plastic moment capacity of the ROPS. The term plastic moment capacity has again been re-introduced to quantify the stiffness

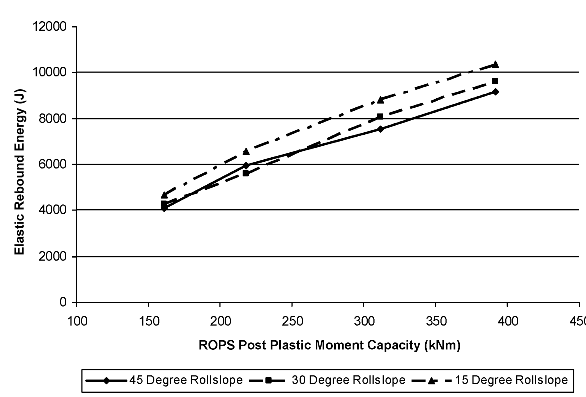

Fig. 13. Elastic rebound energy of ROPS—effects of plastic moment capacity and rollslope angle.

of the ROPS posts. It is clearly evident from this graph that the amount of elastic rebound energy that is released during a rollover impact increases with increasing ROPS post stiffness and is more severe for smaller roll slope angles.

5.5 Dynamic amplifications

The energy absorbed by the K275 ROPS under the established dynamic loading conditions for each stiffness configuration was compared with the corresponding energy absorption capabilities under static loads (Clark, 2006a). This was done for a given deflection and then repeated at regular intervals. The mean dynamic amplifications were then determined for each roll slope angle and ROPS post stiffness. The results are shown in Figure 14 and emphasize that there are dynamic amplifications in the energy absorbed by all ROPS models and that this can be as much as 25% compared to the corresponding static energy-absorbing capabilities. This can be attributed to the influence of the strain rate and inertia effects arising from the input KE. These findings suggest that a much greater energy demand will be placed on ROPS during a dynamic rollover event as compared with energy absorption criteria present within current ROPS performance standards.

5.6 Effect of impact duration—transient pulse loading

It is known that the surface properties have an influence on the impact duration of a rollover. To further enhance the understanding of the impact response of rollover protective structures, a dynamic study was performed that involved the use of transient pulse loads. The time duration of the impulse was varied to study rollover impacts that could take place on a variety of surface conditions. In the field of vehicle crashworthiness, impact studies have shown that during frontal collisions, automotive vehicles are subjected to a force distribution that commonly takes the form of an impulse curve. Common impulse curves used for the evaluation of such events may be either haversine, half sine, triangular, or square in shape. The shape of the loading distribution that is placed on ROPS during an impact arising from a sidewards rollover, is unknown and has received little attention by researchers in the open literature. In the absence of such information, an assumption has been made that idealizes the rollover impact as a transient half-sine pulse. The duration of this pulse is an additional parameter that has not been clearly defined by other researchers in this area. Some guidance, however, has been provided by the earthmoving machinery manufacturer Caterpillar, who, during the late 1960's performed a series of full-scale dynamic rollover tests on a variety of earthmoving machines on roll slopes of varying inclination and soil type. Visualization of this video footage suggested that the contact time between the ROPS and the ground during a rollover may lie within the 100 to 300 ms range. Results in the previous section also indicated similar contact times (80 ms–280 ms). Based on this information, a series of transient pulse loads with durations ranging between these limits were developed and applied to the established FE model of the K275 ROPS using the explicit FE code LS-DYNA.

5.6.1 Determination of pulse variables. Using principles of dynamics and with reference to Figure 5c for side roll of a vehicle and its rotation,

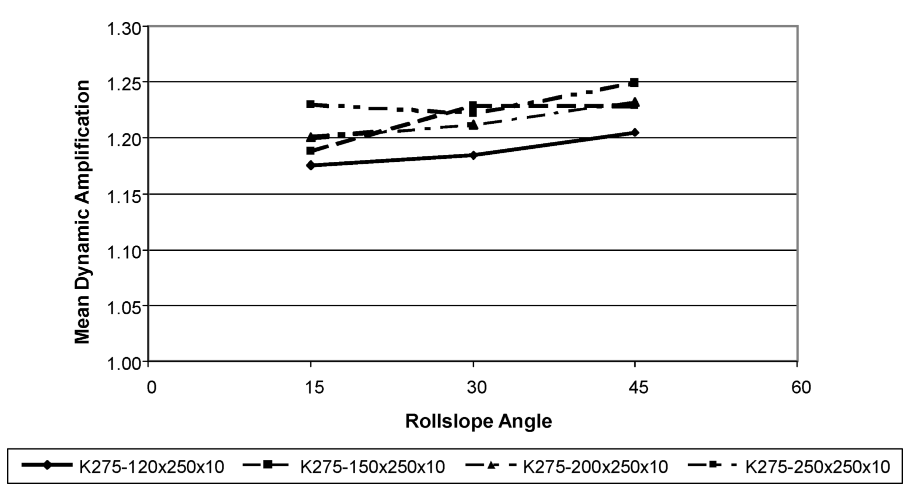

Fig. 14. Dynamic amplification of energy absorbed for different ROPS stiffness and rollslope angle.

Table 2
Summary of peak values of impulse loads

		15°		*30°*		*45°*	
Time (ms)	*BD (m)*	$\Delta I\omega_d$ *(kgm²/s)*	*A (kN)*	$\Delta I\omega_d$ *(kgm²/s)*	*A (kN)*	$\Delta I\omega_d$ *(kgm²/s)*	*A (kN)*
100	2.461	270,847	1,728	330,018	2,106	381,252	2,433
150	2.461	270,847	1,152	330,018	1,404	381,252	1,622
200	2.461	270,847	864	330,018	1,053	381,252	1,217
250	2.461	270,847	692	330,018	842	381,252	974
300	2.461	270,847	576	330,018	702	381,252	812

$$F(t)x(BD) = \mathrm{d}/\mathrm{d}t(I\omega_D), \tag{11a}$$

where I is the polar moment of inertia of the rotating body, ω the angular velocity, $\mathrm{d}/\mathrm{d}t(I\omega_D)$ the rate of change in angular momentum, $F(t)$ is the impact force on the body, and (BD) the moment arm.

For the assumed half-sine transient pulse, this impact force is given by

$$F(t) = A\sin(\pi t/T), \tag{11b}$$

where t is time, T is the duration of the pulse (= contact time), and A the amplitude.

Using Equations (11a,b) and integrating across the time of contact, the amplitude A can be determined and then the expression for the impact force $F(t)$ takes the form

$$F(t) = \frac{\pi \Delta I\omega_D}{2TBD}\left(\sin\left(\frac{\pi t}{T}\right)\right). \tag{12}$$

This equation can be used to model a number of pulses with different durations and will enable the impact response of the ROPS on surface profiles with varying conditions to be assessed.

5.6.2 FE model. The FE model was similar to the one treated earlier and it was subjected to a series of dynamic pulse loads. For this investigation, a 150 × 250 × 10 RHS and a 250 × 250 × 12 RHS were used for the posts and beam of the ROPS, respectively. As before the Hughes–Liu shell element with a mesh density of 20 mm were used to model the ROPS, two material models were used to simulate the response of the ROPS under the applied pulse loads. The first model was the LS-DYNA nonlinear material model MAT_PIECEWISE_LINEAR_ PLASTICITY, which was applied to all the ROPS elements, except those that were within close proximity to the loading zone. For the loading zone region, an elastic strip was incorporated into the model to avoid excessive deformation of the ROPS material. Implementation of this strip involved specifying the LS-DYNA material model MAT_ELASTIC to all elements within this region. Similar to the previous dynamic analysis in Section 5, elastic material properties of density $\rho = 7{,}850\ \mathrm{kg/m^3}$, Elastic modulus $E = 200{,}000$ Mpa, and Poisson's ratio $\nu = 0.3$ were assumed. Strain rate effects, Cowper Symonds relations, and the boundary conditions were identical to those used earlier.

Loading of the ROPS involved application of a face pressure load to the outer surface of the top corner of the ROPS over a 250 mm × 250 mm zone. The intensity of

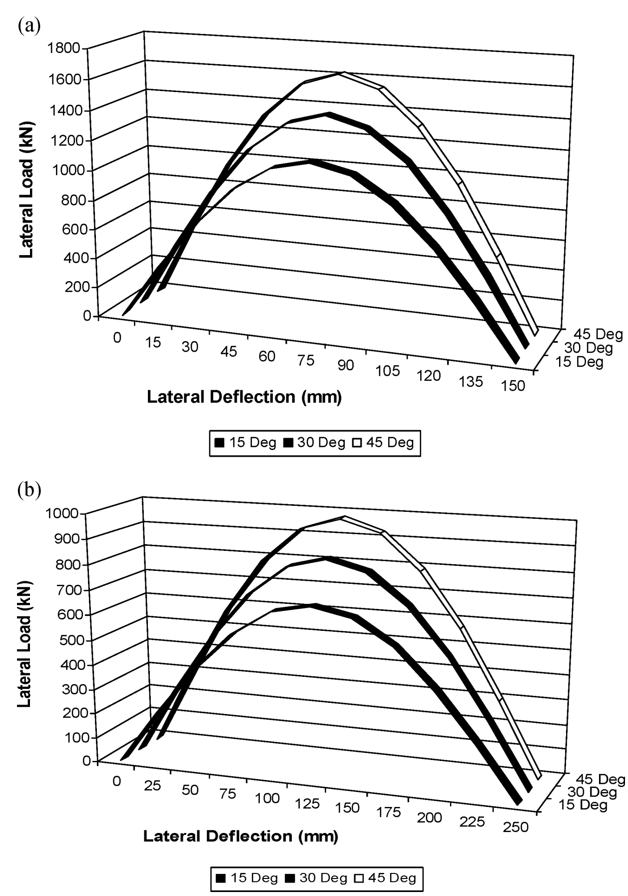

Fig. 15. (a) 150 ms load pulses; (b) 250 ms load pulses.

the face pressure was dependent on the time of contact used for the pulse load. The contact time of the pulse was varied between 100 and 300 ms to account for differing surface conditions that may be experienced by the ROPS during rollovers on roll slopes with inclinations ranging between 15° and 45°. Table 2 provides a summary of the peak values of the force $F(t)$ (i.e., the amplitude A in equation (11b)) that were applied to the ROPS model. Figure 15a and b shows the transient load pulses for 150 mm and 250 mm contact times. The pulses for other contact times were similar. The FE model was subjected to each dynamic pulse load for the defined roll slope inclinations giving rise to a total of 15 FE simulations. There was no need for any contact definition as loading of the ROPS was performed through the application of face pressures only. The output requests from LS-DYNA involved monitoring the displacements of certain nodes located on the ROPS in association with the recording of the base reactions forces that were determined for the base perimeter nodes of each post. Energy data and visualization output data were also recorded for each simulation.

5.6.3 Results from transient load analysis. Table 2 indicates that the intensity of the applied load (A) is most severe for impacts of short duration. For certain pulse durations, the peak force intensity of the pulse was calculated to be well above the collapse load of the ROPS, which resulted in premature failure. To account for this, a termination condition was introduced, which allowed the analysis to be prematurely stopped once the zone of the DLV had been violated and the ROPS was no longer able to provide protection to the vehicle's operator. For this particular ROPS configuration, this deflection limitation was set to 500 mm. Each model was analyzed for the load pulses described above and the load deflection behavior of the ROPS was plotted accordingly and is displayed in Figures 16a–c. These graphs show that for short duration impulses, the deflection limit of 500 mm was impeded during each analysis and that the responses are similar to those experienced by a simple fixed base framed structure under a sidewards applied static force. The interesting difference in this response is the second peak that takes place in the load deflection response of the model prior to reaching the DLV deflection limitation.

(a)
(b)
(c)

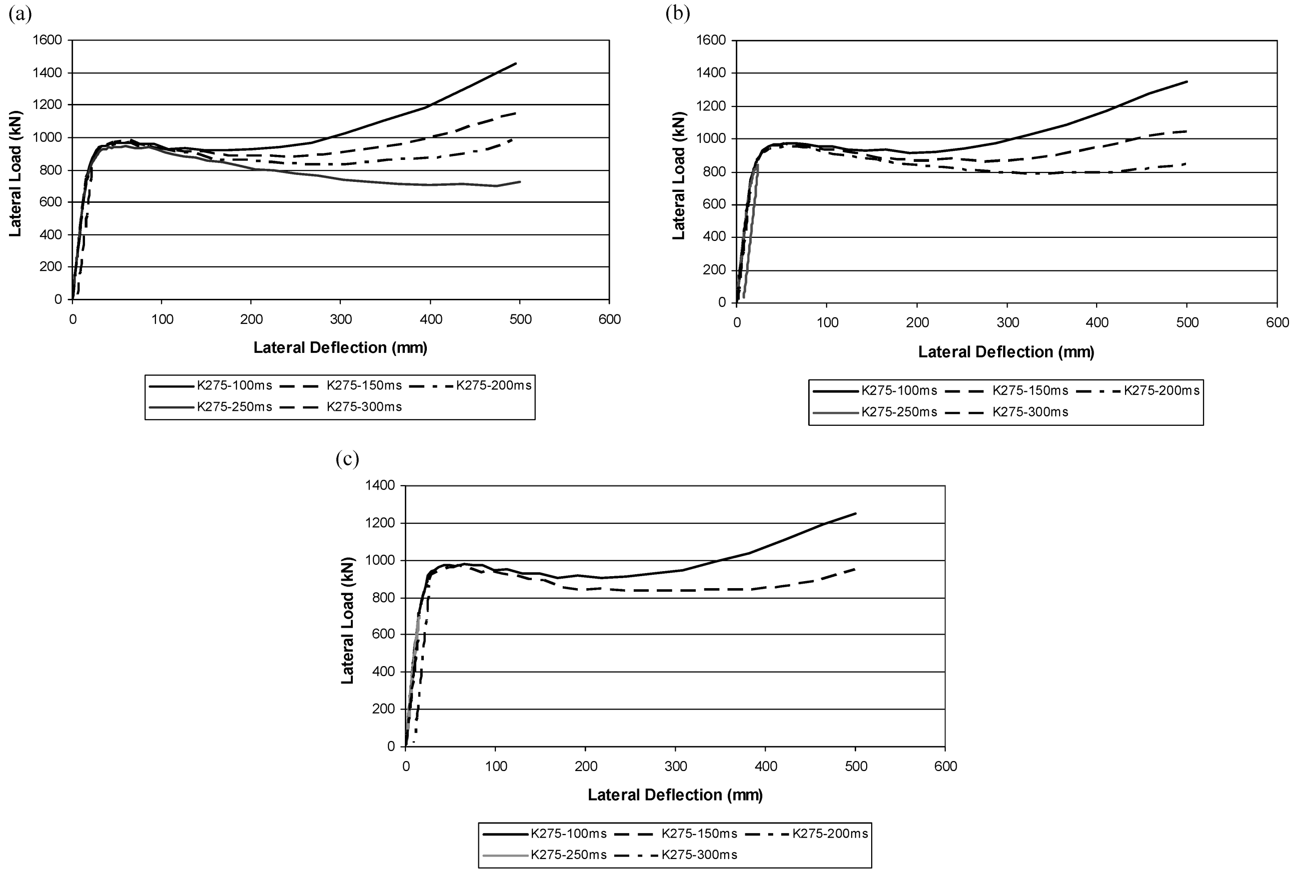

Fig. 16. (a) Load deflection response for 45° rollslope; (b) load deflection response for 30° rollslope; (c) load deflection response for 15° rollslope.

This behavior is believed to be a second-order effect that has been characterized by the extensive plastic deformation sustained by the ROPS during this loading sequence in association with the influence of strain rate effects on the model. Von Mises stress distribution throughout the ROPS and the extent of the plastic deformation experienced by the ROPS for a 100 ms impulse on a 30° roll slope were plotted, and the results were similar to those shown in Figure 9. Plastic hinges developed at the top and base of each post.

The energy absorbed by the ROPS for each case is given in Table 3 and illustrated in Figure 17. Typically, the trend that may be depicted from each of these graphs is that the short duration pulses that are characteristic of impacts that would occur on hard surfaces will result in significant plastic deformation that is characterized by a high force/deflection demand and a corresponding large amount of energy absorption. For large duration pulses that are characteristic of softer surface impacts, the force/ deflection demand placed on the ROPS will be small and consequently the energy-absorbing capacity of the structure will also be small. For events such as this, the soil will be forced to absorb more of the impact energy, whereas for impacts on firm surfaces, the ROPS will be forced to absorb a much larger proportion of the rollover energy. The energy absorbed under larger duration (250 ms and 300 ms) pulses are too small to be seen clearly in this figure.

Figure 17 shows that the energy absorbed by the ROPS is a decreasing function of the pulse duration and highlights that much larger energy demands are placed on ROPS during an impact on a firm soil when compared to a corresponding impact on a softer soil. The other noticeable trend that is evident from this graph is a slight increase in the energy absorbing capacity of ROPS for an impact occurring on a steeper roll slope. The reason for this increase may be attributed to the influence of inertia effects as a higher impact velocity is associated with a steeper roll slope. The influence of this parameter may also be distinguished through reference to the Figure 16a–c, where the second peak in the load carrying capacity of the ROPS increases with increasing roll slope inclination, further emphasizing the possible influence of the strain rate sensitivity of the ROPS material.

Table 3
Energy absorption levels under transient pulse loads

Time (ms)	*15° Rollslope*	*30° Rollslope*	*45° Rollslope*
100	389,945 J	392,231 J	425,365 J
150	367,052 J	372,772 J	396,527 J
200	14,811 J	361,993 J	371,378 J
250	5,410 J	12,811 J	363,511 J
300	4,163 J	5,823 J	10,641 J

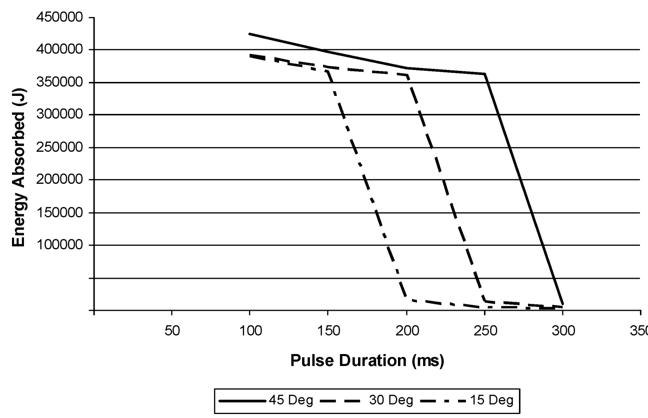

Fig. 17. Energy vs. impulse duration for varying rollslope angles and impact durations.

6 CONCLUSIONS

FE techniques have been used to carry out dynamic impact simulations on ROPS that would be characteristic of those encountered during a sideward rollover of an earthmoving vehicle on a slope. Dynamic loads were developed based on conservation of angular momentum principles. The results from the study showed some interesting and important trends.

6.1 Energy absorption

The present approach resulted in the ROPS energy-absorption criteria that exceeded the requirements of the current Australian standard by as much as 190%. This figure may seem alarming and may question the adequacy of the current Australian standard, however, it must be noted that the approach in this article is approximate and does not account for any further energy absorption by other parts of the vehicle. Moreover, the exact philosophy behind the energy absorption principles in the standard is not clear, which makes its accuracy difficult to question. Aside from accuracy of either method, the present results showed that the method of energy dissipation under dynamic loading was similar to that under static loads.

For roll slope angles of 15° and 30° it was found that ROPS proportioned according to the minimum code requirement could successfully withstand the initial impact of a sideward rollover. However, when the roll slope angle was increased to 45°, which is outside the scope of the standard, it was found that the DLV would be impeded. Other ROPS models with higher stiffness were found to absorb the energy of the initial impact for all roll slope angles. Although energy absorption levels were significantly larger for each ROPS, the DLV zones were not impeded under the estimated first impact on the roll slopes considered.

6.2 Peak loads and dynamic amplifications in absorbed energy

It was discovered that strain rate effects and inertia influences due to the input KE resulted in significantly higher peak loads for each ROPS frame studied. This increase in load was found to fluctuate during the initial load deflection response. A more accurate assessment however, was made by establishing the amplification of energy absorbed. This dynamic amplification was as much as 25% for the K275 ROPS models treated in this study.

As expected the peak decelerations were found to be an increasing function of ROPS post stiffness and were also more pronounced for steeper roll slope inclinations. This result suggests that a stiffer ROPS may therefore be less desirable for occupant protection as opposed to a more flexible one.

6.3 Ground surface condition and impact duration

Influence of ground surfaces conditions on the impact response of the ROPS was investigated by varying the duration of the impact pulses. It was discovered that shorter duration pulse loads resulted in complete collapse of the ROPS structure and consequently resulted in large energy absorption demands being placed on the ROPS. The influence of the strain rate sensitivity of the ROPS material was found to have only a minor influence on the energy absorption capability of the ROPS, with a general trend indicating that steeper angle impacts resulted in slightly higher levels of energy absorption demand being placed on the ROPS. Long-duration pulse loads were found to place lower energy absorption demands on the ROPS by forcing the ground surface to absorb more of the rollover energy.

Stiffer ROPS had a shorter period of contact, which resulted in a higher level of elastic rebound energy, whereas a more flexible ROPS possessed a longer contact time and was therefore able to dissipate the rollover energy more effectively with much less elastic rebound energy. The larger elastic rebound energy in stiffer ROPS is indicative of possible further rolls. This finding also promotes the use of more flexible rollover protective structures for use as energy-absorbing safety devices.

6.4 Main findings

- ROPS proportioned based on the minimum static load provisions of the ROPS standard AS2294 (1997) could adequately sustain an initial sidewards impact on a firm roll slope with an inclination as high as 30° without DLV violation.
- Use of an overly stiff ROPS resulted in the generation of high peak decelerations and reaction forces that may be detrimental to the occupant's chances of survival during a rollover.
- ROPS post stiffness played an important roll in controlling its energy-absorbing capacity.
- Mean dynamic amplification in energy absorbed increased with increasing roll slope angle and this amount varied from about 17% to 25% for the ROPS cases treated.
- The power and feasibility of using analytical techniques for evaluating ROPS performance, which was one of the main aims of the QUT research project, has been demonstrated.

REFERENCES

Australian Standard (1997), Earth-moving machinery—protective structures, Parts 1–4, AS2294a, Sydney, NSW, Australia.

Carney III, J. F. (1993), Motorway impact attenuation devices: past, present and future, in N. Jones and T. Wierzbicki (eds.), *Structural Crashworthiness and Failure*, Elsevier, London & New York.

Chou, C. C., Wu, F., Gu, L. & Wu, S. R. (1998), A review of mathematical models for rollover simulations, crashworthiness, occupant protection and biomechanics in transportation systems, AMD –Vol. 230/BED-Vol. 41, USA.

Clark, B. J. (2006a), The behaviour of rollover protective structures subjected to static and dynamic loading conditions. Ph.D. thesis, QUT, Brisbane, Australia.

Clark, B. J., Thambiratnam, D. P. & Perera, N. J. (2006b), Analytical & experimental investigation of a rollover protective structure, *Journal of the Institution of Structural Engineers, U.K.*, Special Queensland Edition, January, **84**(1), 29–34.

Cobb, L. J. (1976), ROPS force and energy absorption from simulated overturn analysis, SAE Paper 760691, IL, USA.

Harris, J. R., Mucino, V. H., Etherton, J. R., Snyder, K. A. & Means, K. H. (2000), Finite element modeling of ROPS in static testing and rear overturns, *Journal of Agricultural Safety and Health*, **6**(3), 215–225.

Ho, H. M. (1994), Vehicle rollover (ROPS) and falling-object (FOPS) protective structures. Ph.D. thesis, UMIST. Manchester, UK.

Hunckler, C. J., Purdy, R. J. & Austin, R. D. (1985), Non-linear analysis of the terex scraper rollover protective cab, SAE Paper 850788, IL, USA.

Johnson, G. R. (2001), Experimental and numerical investigation into impact bending collapse of rectangular hollow sections Ph.D. Thesis, UTS, Sydeney, NSW, Australia.

Kim, T. H. & Reid, S. R. (2001), Multiaxial softening hinge model for tubular vehicle rollover protective structures, *Mechanical Sciences*, **43**, 2147–2170.

Kacigin, V. V. & Guskov, V. V. (1968), The basis of tractor performance theory, *Journal of Terra-Mechanics*, **5**(3), 43–66.

Klose, G. L. (1969), Engineering basics of rollover protective structures, SAE Paper 690569, IL, USA.

Lu, Guoxing & Yu, Tongxi (2000), *Energy Absorption of Structures and Materials*, Woodhead Publishing Limited, Cambridge, England.

Srivastava, A. K., Rehkugler, G. E. & Masmore, B. J. (1978), Similitude modelling applied to ROPS testing, *Transactions of the American Society of Agricultural Engineers*, **24**(4), 633–645.

Surface Vehicle Standard. (1994), Performance criteria for rollover protective structures for construction, earthmoving, forestry, and mining machines, surface vehicle standard SAE J1040, SAE International, PA, USA.

Swan, S. A. (1988), Rollover protective structure (ROPS) performance criteria for large mobile mining equipment, information circular 9209, US, Bureau of Mines.

Tomas, J. A., Altamore, P. & Sheffield, S. R. (1997), Computer simulation of ROPS for earthmoving vehicles, *Quarry Magazine* (July), 31–36.

Watson, E. M. (1967), The structural testing of tractor safety frames, New Zealand Agricultural Engineering Institute Research Publication R/1.